Structure and function of the endothelial surface layer: unraveling the nanoarchitecture of biological surfaces

Brandon P. Reines[1,2] and Barry W. Ninham[2]

[1]Department of Biomedical Informatics, University of Pittsburgh School of Medicine, 5607 Baum Blvd., Pittsburgh, PA 15206, USA and [2]Department of Applied Mathematics, Research School of Physical Sciences, Australian National University, Canberra, A.C.T. 0200, Australia

Abstract

Among the unsolved mysteries of modern biology is the nature of a lining of blood vessels called the 'endothelial surface layer' or ESL. In venous micro-vessels, it is half a micron in thickness. The ESL is 10 times thicker than the endothelial glycocalyx (eGC) at its base, has been presumed to be comprised mainly of water, yet is rigid enough to exclude red blood cells. How is this possible? Developments in physical chemistry suggest that the venous ESL is actually comprised of nanobubbles of CO_2, generated from tissue metabolism, in a foam nucleated in the eGC. For arteries, the ESL is dominated by nanobubbles of O_2 and N_2 from inspired air. The bubbles of the foam are separated and stabilized by thin layers of serum electrolyte and proteins, and a palisade of charged polymer strands of the eGC. The ESL seems to be a respiratory organ contiguous with the flowing blood, an extension of, and a 'lung' in miniature. This interpretation may have far-reaching consequences for physiology.

Introduction and background: the enigmatic endothelial surface layer (ESL)

Although we understand a lot about molecular events inside cells, particularly about nuclear DNA, our grasp of phenomena occurring at the surface of cells and of collections of cells is much less sure. In particular, we have only recently begun to understand how the surface of alveoli in the lungs really operates in order to facilitate breathing (Larsson *et al.*, 1999). But how the surface of blood vessel linings maintains necessary rheological characteristics for blood flow has largely remained a mystery. The inside or 'lumen' of blood vessels is lined first and foremost by endothelial cells which face the flowing blood. Although the endothelial cells themselves are fairly well understood as biological entities, virtually all of the loosely-adherent non-cellular layers inside of that endothelial lining are very poorly understood, particularly in terms of their physical chemistry. Blood vessels are lined by a very unusual entity which was assumed to be part solid and part liquid, which acts as a cohesive unit, and is known as the endothelial surface layer or ESL (Pries *et al.*, 2000) (see Fig. 1).

In venous microvessels, where most studies have focused, the ESL is approximately 0.5 μm in thickness. Of that, only 50 nm is demonstrably comprised of organic molecules: a predominately polysaccharide mixture of heparan and chondroitin sulfates extending out from the endothelial membrane surface, with hyaluronic acid (HA) loosely associated with, and interior to, those polymeric sulfates. That whole region of relatively compact organic molecules is known as endothelial glycocalyx (eGC). However, the rest of the ESL, a relatively vast 450 nm in width, is 10 times larger: it is the empty region shown as a question mark in Fig. 1, 'anchored' if at all by a vanishingly dilute organic fringe of HA polymers and possibly adsorbed serum proteins (Figs 4–6). In fact, it is so dilute that, if the ESL were truly comprised predominantly of liquid, as is currently presumed, it would contain only a fraction of 0.0007 organic matter! (Secomb *et al.*, 1998). But this is quantitatively absurd, and fails to explain how it is that the exceptionally dilute outer zone of the ESL of venous microvessels has the capacity to exclude red blood cells (RBCs), and to rebound to its original dimensions after passage of large white blood cells (Han *et al.*, 2006) – as if it were a coherent entity. Vascular biologists have attempted to explain these and other anomalies of the ESL by invoking outmoded physical chemical concepts, mainly electrostatic charge operating in high ionic strength biological fluids such as blood (Damiano and Stace, 2002; Curry and Michel, 2019).

The changing face of physical chemistry

The early founders of the cell theory of biology and the physiologists took it as axiomatic that advances in their disciplines had to draw on the enabling fields of the physical sciences. In principle no one would doubt it. But theories of physical chemistry and colloid science in
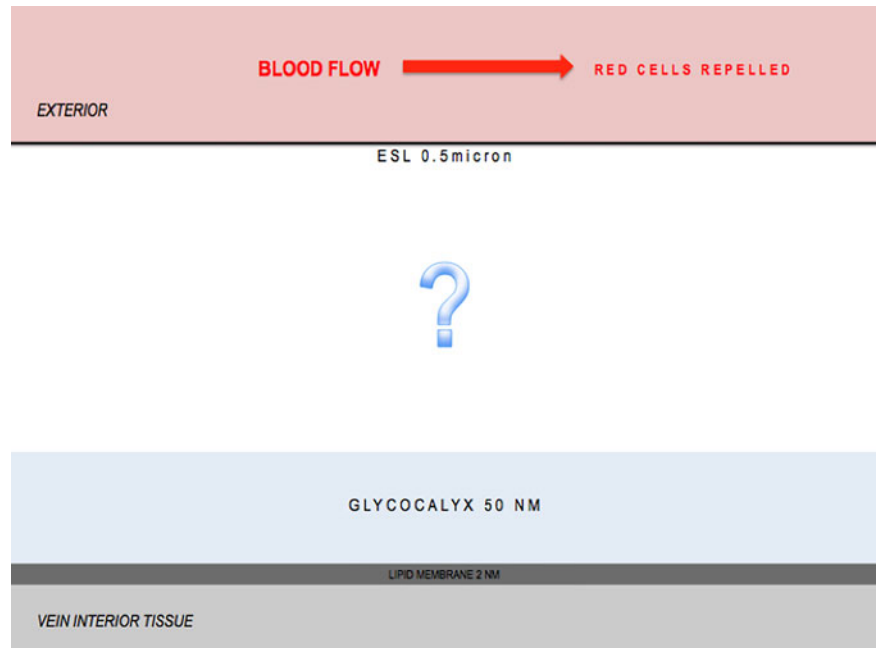
Fig. 1. The mystery of an immeasurably dilute ESL.

aqueous media are now known to have serious flaws that have been dealt with extensively elsewhere (Hyde *et al.*, 1996; Ninham and Nostro, 2010; Ninham, 2017; Ninham *et al.*, 2017a, 2017b, 2017c). The defects in theory are sins of commission, and sins of omission. These developments in our understanding of forces have turned the discipline on its head. However, it turns out that an even more serious omission, the major missing X-factor, the hidden variable, lies in the effects of dissolved gas. This is something totally absent from theory. Recent developments that take this into account do allow new insights into various biological enigmas, including that of the ESL.

The resolution of the problem of pulmonary action discussed below is illustrative. Indeed, the explanation of pulmonary surfactant function and of the alveolar surface layer structure is a backdrop for untangling the ESL problem.

Pulmonary 'surfactant': new understanding

For a century (Pattle, 1958), respiratory physiologists clung to the notion that pulmonary surfactants 'work' by forming a monolayer and/or a multi-bilayer lipid structure called tubular myelin at the air–fluid interface above the alveolar epithelium. However, this 'surface tension' model was shown to be physically impossible (Bangham, 1992). Therefore, the question how lung surfactants at the surface of alveoli take in O_2 and N_2, followed by a re-opening after exhalation of CO_2 and H_2O remained unanswered. Cryo-transmission electron microscopy (TEM) techniques revealed the real structure and mechanism of function of the surface lining of the lung (Larsson *et al.*, 1999; Scarpelli, 2003; Follows *et al.*, 2007; Pérez-Gil, 2008; Larsson and Larsson, 2014; Olmeda *et al.*, 2015). The alveolar surface is comprised of 90% by the membrane-forming lipid phosphatidyl choline and several specialized surfactant proteins called A–D.

The self-assembled structure that does the trick is a prime example of non-Euclidean geometries (Hyde, 1997). Cryo-TEM on freshly opened live rabbit lungs, in 1999 (Larsson *et al.*, 1999), revealed pulmonary surfactant to be a complex three-dimensional structure. 'A single lipid bilayer is curved in space, forming a tetragonal structure (CLP) with tubular units, the walls of which are close to planar and parallel to two orthogonal directions' (Larsson *et al.*, 1999; Larsson and Larsson, 2014).

The proteins play an integral part, forming hexamers at the corners of the cubes (with priority over the toy maker Leggo) (see Fig. 2).

This structure opens and closes throughout the lifetime of an individual with virtually no energy cost. It opens to allow influx of O_2 and N_2, followed by refolding accompanied by expulsion of CO_2 and water. Since then, substantially more work has been done (Scarpelli, 2003; Follows *et al.*, 2007; Pérez-Gil, 2008; Larsson and Larsson, 2014; Olmeda *et al.*, 2015). Experimental visualization and theory agree. It is not inconsistent with a view that the alveolar surface network (ASN) consists of a foam of nanobubbles (Pattle, 1958). The ASN is not just the liquid circulating around the nanobubbles in the alveolar foam but includes the bubbles necessarily. (We note that the nanobubbles are partially stabilized even with lung surfactant deficiencies in premature babies, reflecting the bubble–bubble fusion inhibition phenomenon [salt concentration >0.15 M]. See below) The structure of the ASN–lung surfactant region is a helpful background for understanding the ESL.

Elements of a new model of the endothelial surface layer (ESL)

Atmospheric gas: a missing player

A factor completely missed in theory is a physical (as opposed to a biochemical) role for dissolved gas (Mazumdar, 2002; Ninham and Nostro, 2010; Ninham, 2017; Ninham *et al.*, 2017a, 2017b). This hidden variable shows up in several ways:

(1) Molecular gas (O_2, N_2, CO_2) affects long range 'hydrophobic' forces. When a solution is degassed the forces disappear. They switch off (Ninham and Nostro, 2010; Ninham, 2017; Ninham *et al.*, 2017c).
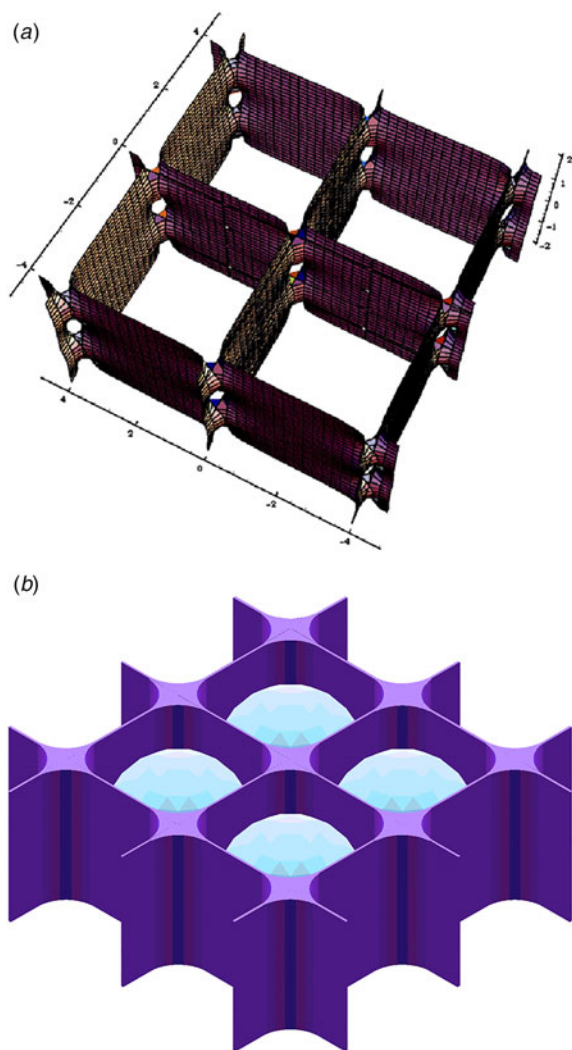
Fig. 2. Actual structure of pulmonary surfactant revealed by cryo-TEM imaging. (A) is reproduced from Larsson et al, 1999 with permission from Springer. Copyright 2002. (B) is a graphical illustration which adds nanobubbles which we postulate must also be present. This remarkably open tetragonal structure is what pulmonary surfactant looks like on full inspiration *in vivo*. Most of the lines consist of phosphatidyl choline, while the peg-like structures at the corners are the surfactant proteins (A–D). This 'action' shot was first revealed by Larsson *et al*. (1999) from cryo-TEM imaging of the alveolar surface of rabbit lungs. On expiration, the open structure collapses to a simple lamellar phase, which creates the impression of extra redundant folds of lipid, which was long construed as 'tubular myelin.' The dimensions of the cubes are about 40 nm, largish nanobubbles Alheshibri, 2016.

(2) Gas in water or physiological fluid exists not only in molecular form; it can be associated to form nanobubbles (Bunkin *et al*., 2011; Alheshibri *et al*., 2016; Yurchenko *et al*., 2016).

(3) Gas bubbles (and nanobubbles) in salt water will not coalesce above a salt concentration of 0.175 molar. This is exactly the ionic strength of the blood (Craig *et al*., 1993*a*, 1993*b*; Henry *et al*., 2007) (see Fig. 3). This still unexplained phenomenon is central to our understanding of the ESL.

(4) Conceptualization and theories of self-assembled structures of lipids, surfactants, oil and electrolyte/water have usually been limited to simple Euclidean geometries: spheres, cylinders and planes. They correspond to micelles, hexagonal phases, vesicles and membranes. But the preferred states of Nature are more often non-Euclidean, bi-continuous structures that
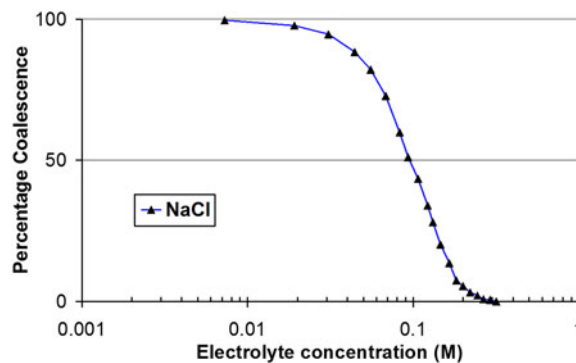
Fig. 3. Experimental measurement of percentage coalescence of bubbles in a column as a function of salt concentration. There is a narrow range centered at physiological concentration over which bubble fusion goes from 100% fusion to no fusion at all.

allow transport (e.g. cubosomes), as in mitochondria, or chloroplasts, or cubic (mesh) phases in conduction of the nervous impulse, and states of supra self-assembly that can transit from one form to another with extravagant ease (Hyde *et al*., 1996; Ninham *et al*., 2017*a*, 2017*b*). The intuition in biology comes from classical theory from which these concepts are absent.

Bubble–bubble fusion inhibition

Blood concentration of NaCl salt is around 0.15 molar, same as that in the Permian ocean from which life emerged (while the effective ionic strength, a more complex entity, is 0.175 M). There are reasons for this. Consider this experiment: bubbles emerge from a frit at the base of a column of water. They collide, fuse and grow bigger as they ascend. The column stays clear. As salt is added, and when the salt concentration reaches 0.175 molar (over a very narrow range) the bubbles no longer fuse. The column becomes opaque and densely packed with small bubbles (Craig *et al*., 1993*a*, 1993*b*; Henry *et al*., 2007) (see Fig. 3).

The phenomenon occurs for a whole range of 1:1 electrolytes at the same concentration. It occurs for multivalent electrolytes at a different concentration, but at the identical ionic strength. In contrast, for a whole range of different salts, e.g. NaAc, it does not occur at all. There are a set of rules that determine which ion pairs 'work,' and which do not, and for mixtures (Henry *et al*., 2007). There are no exceptions. Nobody has any idea why. But the phenomena are indisputable.

Similar phenomena with bubble interactions occur with sugars, but at higher concentrations, typically around and greater than 1 molar (Craig *et al*., 1993*a*, 1993*b*). We can assume that it occurs also with nanobubbles, with sizes varying from several to tens of nanometers. Nanobubbles exist and are stable against fusion at the high ionic strength of blood (Bunkin *et al*., 2011; Alheshibri *et al*., 2016; Yurchenko *et al*., 2016). Such bubbles are further obviously stabilized by surface active solutes, sugars and serum proteins and by surfactants such as lipids.

Strange new forces: polyelectrolytes

Another player missing from theory is the very long-ranged forces of attraction between, and peculiar to, parallel conducting polymers (Richmond *et al*., 1972; Davies *et al*., 1973). These forces
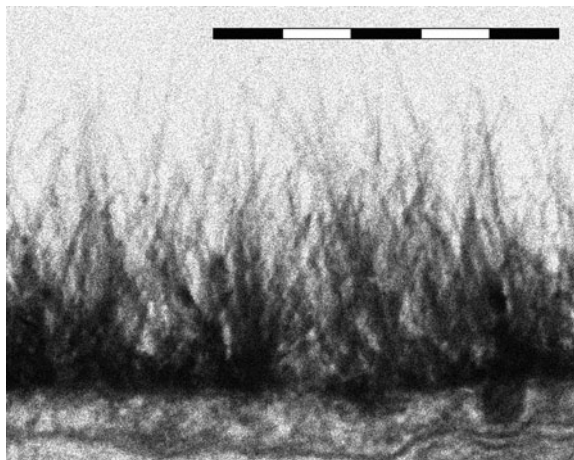
Fig. 4. Electron microscopy image of the endothelial glycocalyx (eGC) in rat myocardial capillary. Reprinted from Fig 1c of van den Berg, B.M., Vink, H., Spaan, J.A. The endothelial glycocalyx protects against myocardial edema. *Circulation Research* 92:592-94, 2003. Bar above image=.5uM.

exist equally for charged (linear) polyelectrolytes of the eGC and DNA (Dekker, 2001; Jimenez-Monroy *et al.*, 2017). They are the analogs of van der Waals forces between atoms or colloidal particles.

The sources of electric current fluctuation correlations that produce the forces are the sheaf of counterions in the electrical double layer that surrounds the charged polymer core. These are very long-ranged, many-body forces. The potential of interaction per unit length is roughly $\sim[1/r(\ln r)^{3/2}]$ where r is the distance between them. They are strictly non-additive and act in concert. Accompanying this strong ordering agency are repulsive electrostatic forces between the polymers. They are much stronger when operating across a vacuum or gas rather than an aqueous medium (as usually assumed in living systems). These forces show up in unrecognized forms. Where they occur they are hidden in terms like 'anomalous water,' a 'fourth phase' of water (Pollack, 2013), and polywater.

The previously inexplicable 'exclusion zone' of the fuel cell polymer, nafion, has recently been explained by these forces (Bunkin *et al.*, 2018). The exclusion zone repels colloidal particles, much as does our ESL. They seem to act in jellyfish to hold them together and in latex polymer suspensions. And probably they are exploited by Nature in spindle structures and ordering in the cell nucleus.

A fortiori, these forces will occur with the highly charged linear polysaccharide polymers of the eGC, most of which are sulfated, including chondroitin sulfate and heparan sulfate. They can explain how polysaccharide strands of the eGC are able to stand upright, perpendicular to the endothelial cell membrane, and parallel to one another in one (open) configuration; and lie down flat as a (closed) coating in another. If separated by gas nanobubbles, not a condensed water medium, the forces are much stronger due to the lack of screening by ions and charged molecules in solution.

Nanobubble model for the endothelial surface layer: a bicontinuous web of polysaccharide strands, water, salt and bubbles held together in a stable foam

First events: eGC–ESL nanobubble interplay

We postulate that first, CO_2, produced as metabolic waste from endothelial cells, diffuses through the microporous 'frit' that constitutes the eGC polymer layer. In so doing, it nucleates nanobubbles of CO_2. The stability of nanobubbles of O_2, CO_2 and N_2

under physiological conditions is assured by the high ionic strength of biological fluids. In the nucleation process, conducting strands of the GC polymer matrix will be teased out, and form a template for the building of the ESL, and a perpendicular scaffolding for the CO_2 nanobubbles (see Fig. 4).

Such linear polyelectrolytes are subject to strong attractive cooperative long-ranged forces that align them. The opposing repulsive electrostatic forces acting across the nanobubbles are also strong (due to absence of ions in gas, as opposed to blood, which would tend to neutralize any such repulsive forces in solution). The balance of these long-ranged forces will be flexible to shear, but stiff against compression, a highly conducting electrical matrix of nanobubbles. In the surface parallel alignment of the eGC, the polymer–polymer repulsive electrostatic interactions are screened by the physiological electrolyte with a short range decay length of 0.8 nm, and coalesce due to the attractive fluctuation forces.

Hypothesis: the ESL structure

With the analogy provided by what we know of lung surfactant structure, we might reasonably postulate that the ESL is comprised predominately of CO_2 and O_2 and O_2/N_2 nanobubbles (with H_2O vapor) in a stable foam. It is a close-packed foam with a very thin bi-continuous layer of aqueous electrolyte and eGC strands separating the CO_2 nanobubbles, which is easy to shear but hard to compress. An essential point is that the nanobubbles in the foam will be prevented from fusion and collapse because the aqueous solution separating them is at or above physiological concentration of ~ 0.15 M salt, and bubbles in an electrolyte concentration above 0.175 M do not fuse. Any shortfall in electrolyte concentration *in vivo* is taken up by the miscellany of accompanying highly charged proteins, High density lipoprotein (HDL)s and Low density lipoproteins (LDL), and act as multiply charged cations to change effective Debye leength and concentration (Mitchell and Ninham, 1978; Kékicheff and Ninham, 1990; Nylander *et al.*, 1994). In arteries, O_2/N_2 nanobubbles are likely predominant, while in veins there is a source of CO_2 that means CO_2 nanobubbles dominate. We imagine there is always a mix of both CO_2 and O_2/N_2 nanobubbles. As for nitrogen/oxygen gas nanobubbles, they have an as yet less certain role (see Fig. 5).

In terms of the nature of the interface between the serum and the ESL, we characterize the ESL as a *periodic steady state structure*. Roughly speaking, we postulate that the number of newly-formed CO_2 nanobubbles diffusing out of endothelial cells is equivalent to the number of such nanobubbles sloughing off the ESL into the flowing blood. We can imagine that the CO_2 nanobubbles at the foam surface keep popping out, in continuous production from CO_2 gas produced inside the endothelial cells and emerging through the eGC 'frit.' Its polymers with a high proportion of sulfate groups are probably impervious to the reactive bicarbonate ion associated with high potassium ion concentration inside. The high external sodium content would act as an energetic solution 'draw' to take the bicarbonate and then CO_2 through gas. In that case, rather than an ion pump, we have a 'gas pump' (see Fig. 6).

The ESL nanobubble model explains paradoxes and anomalies

With a model structure for the ESL now constructed we proceed to challenge it.
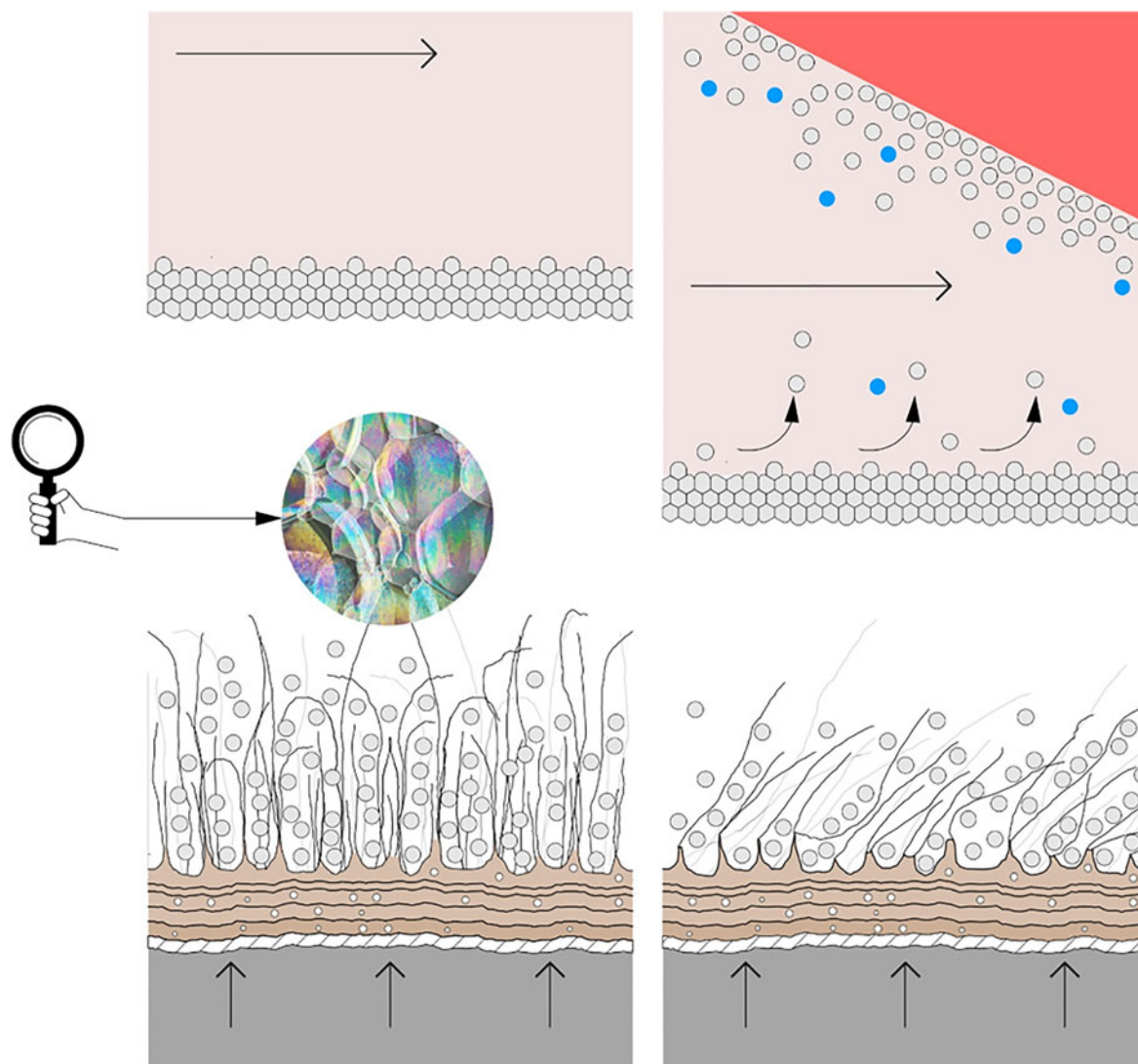
Fig. 5. Diagram of dynamic ESL. A detailed representation of the ESL. The arrows represent CO_2 gas that is passing through the frit formed by the eGC polymeric matrix form a close-packed nanobubble foam illustrated in color. The volume of bicontinuous connected liquid/strand region can be as low as a few percent, cf. Figs 7 and 8. The foam resists compression and repels red cells. On plasma flow the nanobubbles slough off and join the circulation system leaving via the lungs.

The 'arginine paradox' of nitric oxide (NO) production

From a classical biochemical perspective, nitric oxide (NO) is produced enzymatically from the amino acid arginine acting as a substrate for nitric oxide synthase (NOS) enzymes located in or on endothelial cells. However, most measurements *in vitro* and *in vivo* contradict the classical view: the production and biological activity of NO is not determined by cellular arginine at all, but by the amount of *extracellular* arginine (Vukosavljevic *et al*., 2006). The 'arginine paradox' is the fact that despite intracellular physiological concentration of arginine being several hundred micromoles per liter, far exceeding the ~5 μM K_M of eNOS, the acute provision of exogenous arginine still increases NO production.

While a variety of explanations have been put forward to explain the arginine paradox, none has stood the test of time (Shin *et al*., 2011; Elms *et al*., 2013). However, as hydrophobic cavitation and nanobubbles have been shown to have catalytic activity (Nagase *et al*., 1997; Kim *et al*., 2001; Feng et al 2019), the fact that

extracellular arginine is the main determinant of NO production might be simply explained by our nanobubble model of the ESL. Nanobubbles are an abundant source of oxidants and reductants which may potentially catalyze a variety of assumedly enzyme-driven biochemical reactions (Liu *et al*., 2016). The arginine paradox is but one example among many where traditional biochemical thinking about enzyme action comes up short in explaining experimental data. We plan a subsequent essay exploring a new physical chemical view of catalysis.

One question which may arise is: Why would an important signaling molecule like NO, which is apparently capable of powerful effects such as vasodilation, be generated extracellularly and its production left unregulated – at the whim of nanobubble-mediated catalysis? We believe the answer is provided by the recent work by Stamler's group revealing the role played by RBCs in mediating effects which had been thought due to solely to NO, but which are in reality determined by *S*-nitrosothiols (SNOs) (Diesen *et al*., 2008), Stamler has discovered that RBCs take in NO and produce SNOs, which are effectively secreted by
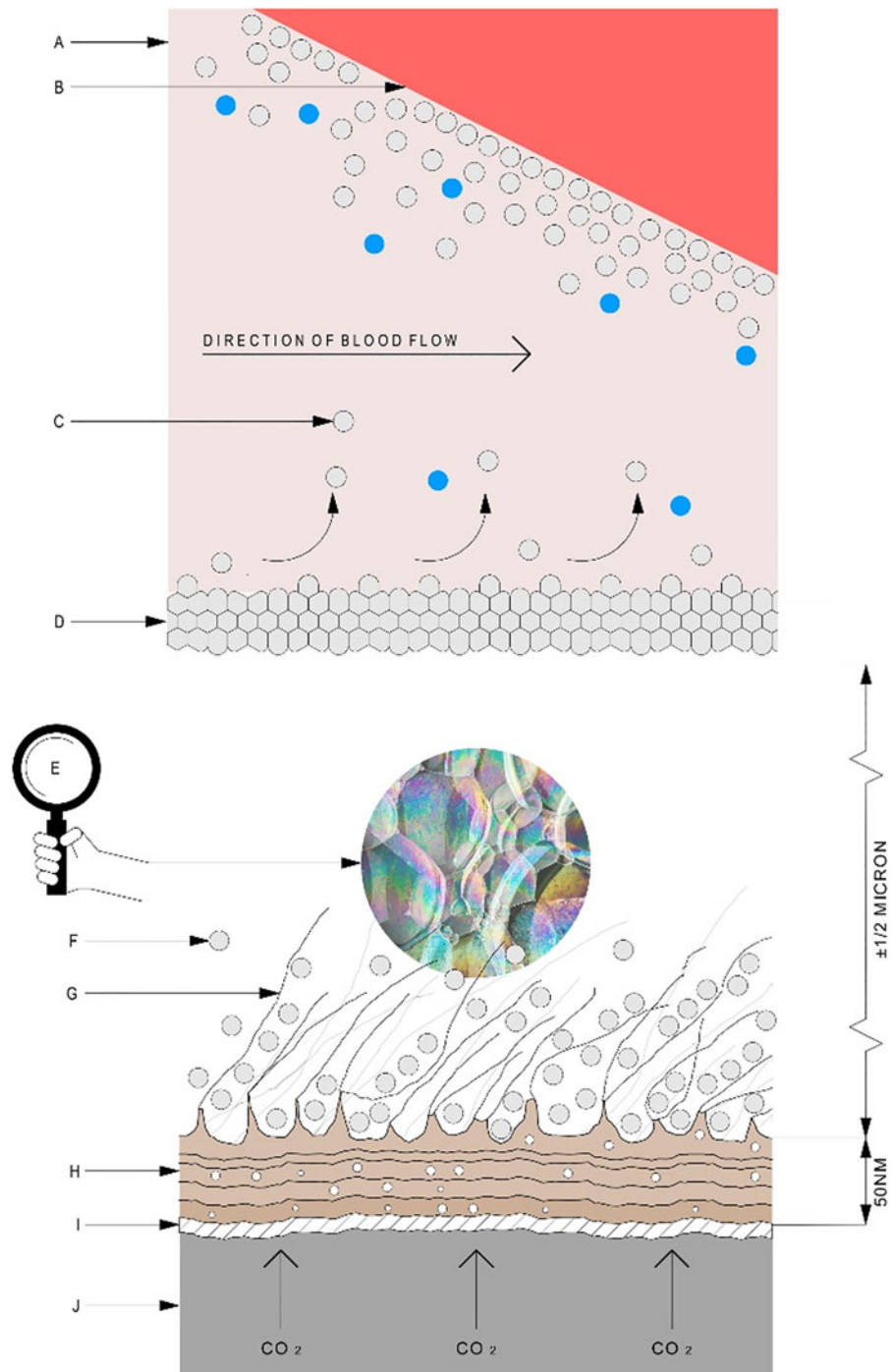
Fig. 6. Labeled structures in ESL of Fig. 5. (a) Blood plasma zone. (b) RBC (6 μm in diameter). (c) Nanobubbles bleb off to join the passing crowd in the plasma on their way to exiting via the lungs. Oxygen/nitrogen cells are indicated in blue. (d) Foam nanobubbles, separated by thin connected layers (∼2 nm) of electrolyte–protein–lipid protein miscellany extend to 0.5 μm. The foam is easy to shear but hard to compress. (e) Flattened nanobubble foam, long range non-additive polyelectrolyte forces and bubble fusion inhibition phenomenon at 0.15 salt stabilizes the continuously regenerated close-packed foam. (f) Nanobubble indicated in gray. (g) Perpendicular glycocalyx polysaccharide strands 'pseudo-seaweed soldiers' in an array, teased out by passage of CO_2 and nucleation of nanobubbles via GC molecular sieve. (h) Glycocalyx (GC), predominately charged polyelectrolytes (50 nm). (i) Cell lipid membrane (2 nm). (j) Cell interior.

the RBCs, and actually induce vasodilation – not NO (Haldar and Stamler, 2013). The coupling of a largely random production of NO with tightly regulated processes inside of RBCs may provide a system which is carefully tailored to local oxygen demands of tissues.

Blood flow, the eGC and nitric oxide production

Han *et al.* write that:

'A problem that has attracted widespread attention is the role of the ESL in transmitting fluid shear stress due to the flowing blood to the intracellular cytoskeleton of the endothelial cell. This problem raises a paradox since it is generally agreed that

the flow within the ESL is negligible and the shear stress at the level of the cell membrane vanishingly small…' (Han *et al.*, 2006).

In a related statement, Thi *et al.* highlight:

'A puzzling and still not understood consequence of eGC (endothelial glycocalyx) degradation was the observation that shear-induced NO production was greatly inhibited without apparent effect on shear-dependent vasodilation due to prostaglandin I2 release' (Thi *et al.*, 2004).

That blood flow must transmit a mechanical signal to the actin cytoskeleton of the endothelial cell derives from the observation that flow does enhance NO release. This tends to dilate vessels and maintain normal blood pressure.

Fig. 7. Dramatic visualization of strands filling with nanobubbles through the eGC Green seaweed and bubbles. iStock by Getty Images, Stock photo ID: 177548832, www.istockphoto.com/au/photo/green-seaweed-and-bubbles-gm177548832-21415810).
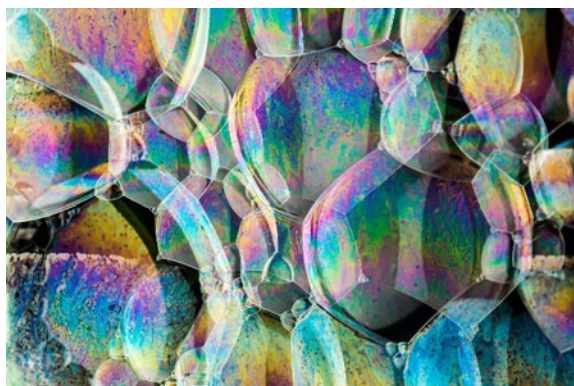
Fig. 8. Magnified section from Figs 5 and 6. To see how the nanobubbles pack more realistically see Karen Uhlenbeck (https://www.nytimes.com/2019/04/08/science/uhlenbeck-bubbles-math-physics.html).

These anomalies include participation of the eGC polysaccharides in NO production, but not for prostaglandin I2-mediated vasodilation. They can be explained as follows: we postulate that molecular NO is produced in most part *extracellularly*.

The hypothesis also explains a third important anomaly: i.e. that NO release does not correlate with actual occupancy of NOS by arginine. Instead, we can reasonably assume that most NO is produced from O_2 in O_2/N_2 nanobubbles. These are known to provide oxidants and reductants which might interact with arginine extracellularly to produce NO (Hickok *et al.*, 2013; Liu *et al.*, 2016; Ahmed *et al.*, 2018). More blood flow would tend to bring in more O_2 nanobubbles, and hence explain the correlation between increased flow, NO and vasodilation.

Soft polysaccharide strands of endothelial glycocalyx stiffen up

Although the eGC is often termed 'gel-like,' most observations show that it is surprisingly soft, more like a bed of sea grass (McLane *et al.*, 2013; van Oosten and Janmey, 2013). Such metaphors, although impressionistic, are sometimes helpful for understanding the nature of the eGC (see, e.g. Fig. 7).

Suggestively, it sometimes has been seen to show a more refined structure, like bundles of rice plants in a paddy field in regular arrays (Squire *et al.*, 2001). How such strands are able to

stand up at all, while the main body of the eGC consists of multiple layers parallel to the cell surface was an enigma of the eGC/ESL system. The explanation of this curious phenomenon has been given in the section 'Elements of a new model of the endothelial surface layer (ESL).' It depends on our long range attractive forces. The same forces have been shown recently to be the source of a similarly anomalous 'exclusion zone' in nafion, a fuel cell polymer which is also a sulfonated polymer (Bunkin *et al.*, 2018).

Brief digression and technical comment: similarities with nafion

Major eGC polysaccharide polymeric components are heparan sulfate $[C_{12}H_{19}NO_{20}S_3]_n$, chondroitin sulfate $[C_{14}H_{21}N_{15}S]_n$ and HA $[C_{14}H_{21}NO_{11}]_n$, with HA as the only non-sulfated and non-cell-bound polymer. The first two have high negatively charged sulfate groups. The effective negative charge of these polyelectrolytes is reduced by binding of sodium ions (80–90%) for electrostatic interactions between the polymers in solution: the strands do not repel each other significantly in a medium with electrolytes. They do have strong short ranged repulsive hydration forces between them. This is one reason the eGC is soft and a good lubricant. The other reason is that HA is also charged with carboxylate residues, and a spacer for the hydrocarbon moieties of heparan sulfate (HS) and chondroiton sulfate (CS).

These polymers share characteristics with the hydrogen fuel cell polymer nafion, made up of multiple tetrafluoroethylenes, rather than sialic acid moieties with terminal SO_3H sulfonic groups, which is to some extent a model for ESL barrier properties (Bunkin *et al.*, 2018). The fuel cell properties of nafion may be shared by the eGC, especially electrical conductance.

How the ESL can be exceptionally dilute yet act as a coherent structure

A confusing number cited in the literature is that the ESL above the eGC contains fractional organic matter of 0.0007, i.e. it is immeasurably dilute (Secomb *et al.*, 1998; Pries *et al.*, 2000). It is impossible to conceive of how a surface layer that is 99.9993% water – and/or space – can exclude RBCs and bounce back to original volume in about half a second after passage of relatively large leukocytes (Han *et al.*, 2006).

The matter is straightforwardly resolved if the ESL is actually a close-packed foam with a very thin bi-continuous layer of aqueous electrolyte and eGC strands separating the CO_2 nanobubbles (see Figs 5 and 6). The aqueous portion of such a close-packed foam can be as low as 0.05% of the whole ESL volume. Then the calculated mean fraction of organic matter in the thin film of water surrounding the foam bubbles drops to a more reasonable ca. 0.14%. Similar artifacts, e.g. on shear stress, and compressibility disappear with the nanobubble model.

The problem refers back to the famous work of Plateau two centuries ago.

For evolution of the transition from spherical bubbles or (oil drops in low external phase emulsions) to close-packed polyhedra at the top of Figs 5 and 6, shown further in Figs 8 and 9 (Lissant, 1966).

'High' versus 'low' salt effects on the ESL

We address here another very peculiar and important phenomenon regarding the effects of salt on the ESL.
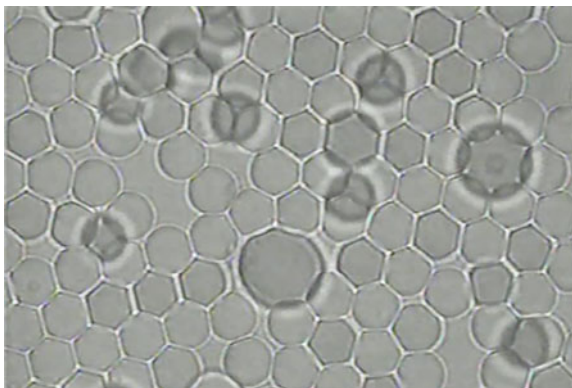
Fig. 9. A different representation of actual close packing of distorted bubbles.

The ESL changes quite dramatically in thickness and rigidity (Oberleithner *et al.*, 2015) when confronted with a change in salt from 'low' to 'high' sodium plasma content: 'low' is 0.133 molar sodium, 'high' is > 0.14 molar. At first sight this is impossible. Electrostatic interactions between ions or ions and surfaces or between surfaces (double layer forces of colloid science) decay with distance L exponentially $\sim\exp(-KL)$ where K is the inverse of the Debye screening distance. For physiological saline this is about 0.8 nm – a couple of water molecules. It cannot be of significance. But it is!

And here is how.

The observation is that increase of Na^+ concentration from 0.133 to 0.14 M had no effect on RBC-endothelium adhesion. Above 0.14 M sudden clear-cut increased adhesion occurred (Oberleithner *et al.*, 2015). Why?

The observed correlation between salt concentration and change in adhesion coincides with the change in bubble–bubble interactions from all fusion to no fusion. For univalent salts the transition is pretty much complete by 0.175 M, cf. Fig. 2. There, per cent bubble-bubble fusion, essentially a step function as for the red cell adhesion experiments is plotted against the concentration of sodium chloride. This (0.175 M) is different from that (0.13 to >0.14 M) of the Oberleithner *et al.* (2015) adhesion experiments. The discrepancy can be reconciled if we recall that for mixtures of salts the transition occurs at the same Debye length. If serum proteins and other dilute multivalent ions in the plasma are taken account of in calculating the Debye length, the range of Na^+ from 0.13 to >0.14 M does span the effective 0.175 M critical strength (Mitchell and Ninham, 1978; Krieg *et al.*, 2014).

The reason for increased adhesion with increased Na^+ is then comprehensible. The ESL foam at the lower (0.13 M Na^+) concentration is a polydisperse and nebulous mixture, sloughing off bubbles. Nothing to adhere to there. Above the critical level (0.14 M Na^+) the ESL nanobubbles are monodisperse, close packed, and provide a firm defined base for adhesion.

The same critical bubble phenomenon with increased Na^+ explains other anomalies in Oberleithner's results (Oberleithner *et al.*, 2015). One is 'an apparent discrepancy between the heparinase-induced eGC damage (stiffness decrease and height decrease) and eGC damage caused by sodium overload (stiffness increase and height decrease) …' (Oberleithner *et al.*, 2007; Oberleithner *et al.*, 2011; Oberleithner *et al.*, 2015). Removal of the perpendicular templating strands of HS and CS in the eGC takes away the stabilizing framework forces; stiffness decreases

and allows more rapid nanobubble escape. Sodium overload enhances bubble mono-dispersity; stiffness increases, and height decreases due to better bubble packing.

ESL phase state, vasodilation, and vascular inflammation: importance of low molecular weight thiols in opening the eGC/ESL

Globally speaking, despite their apparent dissimilarity in biochemical and cellular events, we believe that vasodilation and vascular inflammation are actually closely linked in their physical chemistry. Although molecular entities that open blood vessels and those that induce inflammation are often considered vastly different in their biochemical and cellular effects, it is increasingly apparent that one and the same molecule can have both effects depending on their concentration in blood (e.g. formyl-methionine-leucyl-phenylalanine or fMLP).

In light of that, we believe that the key event in both vasodilation and vascular inflammation with increased permeability to leukocytes is 'opening of the ESL.' We contend that this is very likely due to a *phase change in the entire eGC/ESL* – from a closed lamellar to open cubic or hexagonal 'cubosome' phase. It is difficult to depict this open structure but we would postulate that it is quite close to the quasi-periodic one found in electromicrographs of the eGC/ESL (Squire *et al.*, 2001), with pore sizes of 20–40 nm. This helps explain why it is that, depending on their concentrations *in vivo*, many vasoactive molecules including NO can be beneficial in opening the ESL and the vessel itself, or can induce widespread damage to the vascular wall, when present in unusually high concentrations (Dorward *et al.*, 2015).

Indeed, many vasoactive molecules share an unrecognized structural motif: their formulae contain at least one sulfur-containing moiety. They include *N*-formylmethionine-leucyl-phenylalanine (fMLP), homocysteine, sulfatides (Li *et al.*, 2015), virtually all of the important signaling molecules identified by Stamler (Pawloski *et al.*, 2005; Haldar and Stamler, 2013), and possibly sulfated LDL or multiply thiolated LDL: LDL is special among lipoproteins in binding virtually any sulfur-containing molecule (Nishida and Cogan, 1970; Kim and Nishida, 1977; Kim and Nishida, 1979; Olsson *et al.*, 1997; Camejo *et al.*, 1998; Lundstam *et al.*, 1999). Our model includes the implication that sulfation of polysaccharides in the eGC is critical for maintaining hydration that aligns the strands and prevents them from sticking together. The now-documented sulfur binding capacity of Apolipoprotein B of LDL becomes a key observation explaining how LDL breaches the eGC/ESL barrier, engages its receptor, and, along with facilitated entry of leukocytes, builds atherosclerotic plaques (Kim and Nishida, 1979; Olsson *et al.*, 1997).

Mechanistically, we suspect that the reason so many vasoactive molecules are low molecular weight thiols and may also be known as atherosclerosis risk factors and/or shown to disrupt the eGC/ESL is that they '*compete with*' the hydrated sulfate-Na^+-sulfate '*bridges*' *aligning eGC polysaccharide strands* teased out from the endothelial cell surface (by CO_2). They can do this by inserting their own hydrated sulfur-Na^+-sulfur in place of one holding the strands together. Such low molecular weight thiols would effectively pry the eGC strands apart.

A forced change in packing caused by low molecular weight thiols like fMLPs changes the anisotropic dielectric properties of the conducting eGC layers. This has a large effect on van der Waals forces between approaching neutrophils, for example. The forces can change from repulsive to attractive depending

on anisotropy of the intervening eGC medium liquid-crystal-like strands.

Opening of the ESL by low molecular weight thiols also tends to open blood vessels, i.e. induce vasodilation Some obvious examples of such molecules are Viagra, Levita, and virtually all of the nitrosylated thiols (NSOs) identified by Stamler's group (Haldar and Stamler, 2013).

Their chemical formulae are remarkably similar: fMLP $C_{21}H_{31}N_3O_5S$; Viagra $C_{22}H_{30}N_6O_4S$; and Levita $C_{23}H_{32}N_6O_4S$.

All three are very similar with much the same molecular weight (437 for fMLP) to typical lipids. The sulfate moiety facilitates adsorption in the foam of the ESL and of the eGC. There they induce a transition to a bicontinuous open cubosomal phase that allows uptake of N_2/O_2 nanobubbles and production of nitric oxide.

A further consequence is that these molecules, in their surfactant guise, can in succession be further taken up into cell lipid membranes. There they induce transitions to mesh phases involved in transmission of the nervous impulse, the desired response.

Taurine $C_2H_7NO_3S$ (MW 125) probably dimerizes and have the same physical effects.

Cialis, a precursor erectile drug, $C_{22}H_{19}N_3O_4$ and candesartan, a popular drug for heart disease $C_{24}H_{20}N_6O_3$ will affect the same physical changes and react with sulfate moieties of the eGC polymers.

Low molecular weight thiols induce a phase change in the eGC/ESL

The usual focus on specific formulae and binding sites of such and related molecules masks a more general overarching phenomenon. What is occurring is a phase change triggered by the low molecular weight thiols such as fMLPs in the microstructure of the eGC. This is a re-run of the phase changes in self assembled cell lipid membrane structures that underlies anesthetic action, propagation of the nerve impulse, immuno-suppression by cationic surfactants and pheromone action (Ninham *et al.*, 2017*a*, 2017*b*). Transitions from closed e.g. multiple lamellae, to open bicontinuous phases occur with extravagant ease, induced by cosurfactants or changes in physico-chemical conditions (Ninham *et al.*, 2017*a*, 2017*b*). There is a unifying predictive theory and these matters are well understood.

There is a disconnect in thinking about lipid/surfactant self-assembly *versus* that of polyelectrolyte such as polysaccharide phase behavior (as for the eGC). Yet local curvature *versus* global packing constraints set structure for polyelectrolytes like eGC polysaccharides is governed by the same constraints as for surfactants and lipids. Corresponding to closed lamellae *versus* open cubic phases in lipid/surfactant systems we have closed polymer lamellae-like *versus* open cubosomes in polyelectrolyte systems. The cubosome phases of polymers are very rigid as compared with lamellar states of polymers, besides the obvious unrecognized differences between open and closed physical states. The cubosome literature in cell biology is large and exploited in the pharmaceutical field for drug delivery. Of particular interest in the context of the ESL is the facts that pore sizes are characteristically around 20–40 nm (Squire *et al.*, 2001), that a cubosomal structure for the ESL is very rigid compared with the lamellar state, and the transition can be induced by a wide variety of low molecular weight thiols, small peptides or surfactants. Most share with fMLP the sulfur-containing moiety for hydration compatibility with the ESL polyelectrolytes, facilitating opening of the eGC/ESL.

Discussion: implications for physiology and immunology

Respiratory and vascular physiology are usually treated as separate. The known stability of nanobubbles under physiological conditions suggests now that the two systems are linked. The notion that O_2 is transported bound to hemoglobin is a fact. The notion of a complementary delivery mechanism arises if O_2 (and N_2) nanobubbles exist and are stable in physiological medium. A related, open question is how CO_2, a byproduct of metabolism, exits cells into the circulatory system and on to the lungs for expulsion. It is known that CO_2 diffuses into RBCs, where it is converted to carbonic acid by the enzyme carbonic anhydrase and then converts to HCO_3 (Krieg *et al.*, 2014). But this may not be the only escape route for CO_2. A foam of CO_2 bubbles that form the ESL is another. Such a model resists compression, but is simultaneously susceptible to shear and sloughing off of nanobubbles into blood plasma flow.

At the same time, an optimal level of vessel wall flexibility would be preserved, but not so rigid as to create problems such as limitations on O_2 delivery to tissues and stiffening of vessel walls. The three qualitatively new factors that explain the ESL are: the existence of stable nanobubbles at physiological ionic strength, the phenomenon of bubble–bubble fusion inhibition above 0.175 M, and long range fluctuation forces between polyelectrolytes (Richmond *et al.*, 1972; Davies *et al.*, 1973). The latter, known almost since the discovery of van der Waals forces seems to have fallen through the cracks and been ignored.

Some questions on respiratory and vascular physiology and on immunology can now be revisited. Nature seems to have taken care to put long stretches of positively charged amino acids into hormone-like signaling molecules, like chemokines and cytokines. The function of their cationicity (and specific hydration) was attributed to the requirement that such molecules interact with negatively charged regions of the cell surface, particularly its sulfate-rich glycocalyx. That is a tautology. But an explicit reason associated with nanobubbles can be adduced. The cationic polymer–anionic heparin sulfate complex residues in the eGC would collapse the ESL (Manchanda *et al.*, 2018). The repulsive electrostatic interactions due to the heparin across the (electrolyte-free) nanobubbles that, with the opposing attractive ionic fluctuation forces that stabilize them, are switched off. Therefore, the positive charge matters as long suspected, but not in the way long supposed: in the assumed aqueous system, screening of the charges occurs due to ions, but in the gas eGC/ESL system we propose, the positive charges would definitely collapse the whole system.

It seems that nanobubbles of oxygen, nitrogen and carbon dioxide play a so far previously hidden and complementary role in transport and delivery that is excluded from the conventional canon. It is conceivable that the ESL is part of a connected extension of the lungs like the lymphatic system that we have not previously recognized. The sizes of the compartments in the lungs are around 40 nm, same more or less as those seen in EM images of ESL (20–40 nm) (Reitsma *et al.*, 2007). In this scenario, as is usual in physiology, nitrogen, 80% of atmospheric gas taken in is the odd man out. The arguments above would imply that it too forms nanobubbles, not just a molecular solution, but a mixture with oxygen and they would be a part of the action. The solubility of nitrogen in fact is five times that of oxygen, the connection to the problem of the 'bends' (Craig *et al.*, 1993*a*, 1993*b*, Arieli, 2015; Arieli, 2017).

The structure of the ESL has been a frustrating puzzle. A gallimaufry of enigmas all point to a continuously produced ordered

foam of nanobubbles as the answer. For the ESL the remarkable phenomenon of bubble–bubble fusion inhibition at and around physiological concentration seems an obvious key.

Strong long-ranged polyelectrolyte fluctuation forces seem also to be necessary to explain other curious phenomena – jellyfish, for which the umbrella is variously estimated to be up to 99% water. An extremely dilute matrix permeated by stinging polyelectrolytes just like the ESL seems a more probable explanation. The anomalous exclusion zone at the surface of nafion, the (sulfated) fuel cell polymer, repels colloidal particles or macromolecules, just as does the ESL (Davies *et al.*, 1973; Bunkin *et al.*, 2018). Their shared electrochemical properties with the ESL open up promising new areas.

References

Ahmed AKA, Shi X, Hua L, Manzueta L, Qing W, Marhaba T and Zhang W (2018) Influences of air, oxygen, nitrogen, and carbon dioxide nanobubbles on seed germination and plant growth. *Journal of Agricultural and Food Chemistry* **66**, 5117–5124.

Alheshibri M, Qian J, Jehannin M and Craig VS (2016) A history of nanobubbles. *Langmuir* **32**, 11086–11100.

Alheshibri M, Qian J, Jehannin M and Craig VS (2016) A History of Nanobubbles. *Langmuir: the ACS journal of surfaces and colloids* **32**, 11086–22186.

Arieli R (2015) Was the appearance of surfactants in air breathing vertebrates ultimately the cause of decompression sickness and autoimmune disease? *Respiratory Physiology & Neurobiology* **206**, 15–18.

Arieli R (2017) Nanobubbles form at active hydrophobic spots on the luminal aspect of blood vessels: consequences for decompression illness in diving and possible implications for autoimmune disease – an overview. *Frontiers in Physiology* **8**, 591.

Bangham AD (1992) 'Surface tension' in the lungs. *Nature* **359**, 110.

Bunkin NF, Ninham BW, Ignatiev PS, Kozlov VA, Shkirin AV and Starosvetskij AV (2011) Long-living nanobubbles of dissolved gas in aqueous solutions of salts and erythrocyte suspensions. *Journal of Biophotonics* **4**, 150–164.

Bunkin N, Shkirin A, Kozlov V, Ninham B, Uspenskaya E and Gudkov S (2018) Near-surface structure of Nafion in deuterated water. *The Journal of Chemical Physics* **149**, 164901.

Camejo G, Hurt-Camejo E, Wiklund O and Bondjers G (1998) Association of apo B lipoproteins with arterial proteoglycans: pathological significance and molecular basis. *Atherosclerosis* **139**, 205–222.

Craig V, Ninham B and Pashley R (1993a) Effect of electrolytes on bubble coalescence. *Nature* **364**, 317.

Craig VS, Ninham BW and Pashley RM (1993b) The effect of electrolytes on bubble coalescence in water. *The Journal of Physical Chemistry* **97**, 10192–10197.

Curry FE and Michel CC (2019) The endothelial glycocalyx: barrier functions *versus* red cell hemodynamics: a model of steady state ultrafiltration through a bi-layer formed by a porous outer layer and more selective membrane-associated inner layer. *Biorheology* **57**, 1–18.

Damiano ER and Stace TM (2002) A mechano-electrochemical model of radial deformation of the capillary glycocalyx. *Biophysical Journal* **82**, 1153–1175.

Davies B, Ninham B and Richmond P (1973) Van der Waals forces between thin cylinders: new features due to conduction processes. *The Journal of Chemical Physics* **58**, 744–750.

Dekker CARM (2001) *Electronic Properties of DNA. Physics World*. Bristol: Institute of Physics Publishing. pp. 29–33.

Diesen DL, Hess DT and Stamler JS (2008) Hypoxic vasodilation by red blood cells: evidence for an s-nitrosothiol-based signal. *Circulation Research* **103**, 545–553.

Dorward DA, Lucas CD, Chapman GB, Haslett C, Dhaliwal K and Rossi AG (2015) The role of formylated peptides and formyl peptide receptor 1 in governing neutrophil function during acute inflammation. *American Journal of Pathology* **185**, 1172–1184.

Elms S, Chen F, Wang Y, Qian J, Askari B, Yu Y, Pandey D, Iddings J, Caldwell RB and Fulton DJ (2013) Insights into the arginine paradox: evidence against the importance of subcellular location of arginase and eNOS. *American Journal of Physiology. Heart and Circulatory Physiology* **305**, H651–H666.

Feng B, Sosa RP, Mårtensson AKF, Jiang K, Tong A, Dorfman KD, Takahashi M, Lincoln P, Bustamante CJ, Westerlund F and Nordén B (2019) Hydrophobic catalysis and a potential biological role of DNA unstacking induced by environment effects. *Proceedings of the National Academy of Sciences of the United States of America* **116**, 17169–34343.

Follows D, Tiberg F, Thomas R and Larsson M (2007) Multilayers at the surface of solutions of exogenous lung surfactant: direct observation by neutron reflection. *Biochimica et Biophysica Acta (BBA)-Biomembranes* **1768**, 228–235.

Haldar SM and Stamler JS (2013) S-nitrosylation: integrator of cardiovascular performance and oxygen delivery. *Journal of Clinical Investigation* **123**, 101–110.

Han Y, Weinbaum S, Spaan JA and Vink H (2006) Large-deformation analysis of the elastic recoil of fibre layers in a Brinkman medium with application to the endothelial glycocalyx. *Journal of Fluid Mechanics* **554**: 217–235.

Henry CL, Dalton CN, Scruton L and Craig VS (2007) Ion-specific coalescence of bubbles in mixed electrolyte solutions. *The Journal of Physical Chemistry C* **111**, 1015–1023.

Hickok J, Vasudevan D, Jablonski K and Thomas DD (2013) Oxygen dependence of nitric oxide-mediated signalling. *Redox Biology* **1**, 203–209.

Hyde S, Blum Z, Landh T, Lidin S, Ninham B, Andersson S and Larsson K (1996) *The Language of Shape: The Role of Curvature in Condensed Matter: Physics, Chemistry and Biology*. Amsterdam: Elsevier.

Hyde ST, Andersson S, Larsson K, Lidin S, Landh T, Blum Z and Ninham BW (1997) *The Language of Shape: The Role of Curvature in Condensed Matter Physics, Chemistry and Biology*. Amsterdam: Elsevier Science.

Jimenez-Monroy KL, Renaud N, Drijkoningen J, Cortens D, Schouteden K, van Haesendonck C, Guedens WJ, Manca JV, Siebbeles LD, Grozema FC and Wagner PH (2017) High electronic conductance through double-helix DNA molecules with fullerene anchoring groups. *Journal of Physical Chemistry A* **121**, 1182–1188.

Kékicheff P and Ninham B (1990) The double-layer interaction in asymmetric electrolytes. *EPL (Europhysics Letters)* **12**, 471.

Kim YC and Nishida T (1977) Nature of interaction of dextran sulfate with lecithin dispersions and lysolecithin micelles. *Journal of Biological Chemistry* **252**, 1243–1249.

Kim YC and Nishida T (1979) Nature of the interaction of dextran sulfate with high and low density lipoproteins in the presence of Ca^{2+}. *Journal of Biological Chemistry* **254**, 9621–9626.

Kim H, Tuite E, Norden B and Ninham BW (2001) Co-ion dependence of DNA nuclease activity suggests hydrophobic cavitation as a potential source of activation energy. *European Physical Journal E* **4**, 411–417.

Krieg BJ, Taghavi SM, Amidon GL and Amidon GE (2014) *In vivo* predictive dissolution: transport analysis of the CO_2, bicarbonate *in vivo* buffer system. *Journal of Pharmaceutical Sciences* **103**, 3473–3490.

Larsson M and Larsson K (2014) Periodic minimal surface organizations of the lipid bilayer at the lung surface and in cubic cytomembrane assemblies. *Advances in Colloid and Interface Science* **205**, 68–73.

Larsson M, Larsson K, Andersson S, Kakhar J, Nylander T, Ninham B and Wollmer P (1999) The alveolar surface structure: transformation from a liposome-like dispersion into a tetragonal CLP bilayer phase. *Journal of Dispersion Science and Technology* **20**, 1–12.

Li G, Hu R, Gu J and Wu HZ (2015) Relationship between carotid artery atherosclerosis and sulfatide in hypertensive patients. *Genetics and Molecular Research* **14**, 4840–4846.

Lissant KJ (1966) The geometry of high-internal-phase-ratio emulsions. *Journal of Colloid and Interface Science* **22**, 462–468.

Liu S, Oshita S, Kawabata S, Makino Y and Yoshimoto T (2016) Identification of ROS produced by nanobubbles and their positive and negative effects on vegetable seed germination. *Langmuir* **32**, 11295–11302.

Lundstam U, Hurt-Camejo E, Olsson G, Sartipy P, Camejo G and Wiklund O (1999) Proteoglycans contribution to association of Lp(a) and LDL with smooth muscle cell extracellular matrix. *Arteriosclerosis Thrombosis and Vascular Biology* **19**, 1162–1167.

Manchanda K, Kolarova H, Kerkenpass C, Mollenhauer M, Vitecek J, Rudolph V, Kubala L, Baldus S, Adam M and Klinke A (2018) MPO (myeloperoxidase) reduces endothelial glycocalyx thickness dependent on its cationic charge. *Arteriosclerosis Thrombosis and Vascular Biology* **38**, 1859–1867.

Mazumdar PM (2002) *Species and Specificity: An Interpretation of the History of Immunology*. Cambridge: Cambridge University Press.

McLane LT, Chang P, Granqvist A, Boehm H, Kramer A, Scrimgeour J and Curtis JE (2013) Spatial organization and mechanical properties of the pericellular matrix on chondrocytes. *Biophysical Journal* **104**, 986–996.

Mitchell DJ and Ninham BW (1978) Range of the screened Coulomb interaction in electrolytes and double layer problems. *Chemical Physics Letters* **53**, 397–399.

Nagase S, Takemura K, Ueda A, Hirayama A, Aoyagi K, Kondoh M, Koyama A (1997) A novel nonenzymatic pathway for the generation of nitric oxide by the reaction of hydrogen peroxide and D- or L-arginine. *Biochemical and Biophysical Research Communications* **233**(1), 150–153.

Ninham BW (2017) The biological/physical sciences divide, and the age of unreason. *Substantia* **1**, 7–24.

Ninham BW and Nostro PL (2010) *Molecular Forces and Self Assembly: in Colloid, Nano Sciences and Biology*. Cambridge: Cambridge University Press.

Ninham BW, Larsson K and Lo Nostro P (2017a) Two sides of the coin. Part 1. Lipid and surfactant self-assembly revisited. *Colloids and Surfaces. B, Biointerfaces* **152**, 326–338.

Ninham BW, Larsson K and Nostro PL (2017b) Two sides of the coin. Part 2. Colloid and surface science meets real biointerfaces. *Colloids and Surfaces B: Biointerfaces* **159**, 394–404.

Ninham BW, Pashley RM and Nostro PL (2017c) Surface forces: changing concepts and complexity with dissolved gas, bubbles, salt and heat. *Current Opinion in Colloid & Interface Science* **27**, 25–32.

Nishida T and Cogan U (1970) Nature of the interaction of dextran sulfate with low density lipoproteins of plasma. *Journal of Biological Chemistry* **245**, 4689–4697.

Nylander T, Kékicheff P and Ninham BW (1994) The effect of solution behavior of insulin on interactions between adsorbed layers of insulin. *Journal of Colloid and Interface Science* **164**, 136–150.

Oberleithner H, Riethmuller C, Schillers H, MacGregor GA, de Wardener HE and Hausberg M (2007) Plasma sodium stiffens vascular endothelium and reduces nitric oxide release. *Proceedings of the National Academy of Sciences of the United States of America* **104**, 16281–16286.

Oberleithner H, Peters W, Kusche-Vihrog K, Korte S, Schillers H, Kliche K and Oberleithner K (2011) Salt overload damages the glycocalyx sodium barrier of vascular endothelium. *Pflugers Archiv* **462**, 519–528.

Oberleithner H, Walte M and Kusche-Vihrog K (2015) Sodium renders endothelial cells sticky for red blood cells. *Frontiers in Physiology* **6**, 188.

Olmeda B, García-Álvarez B, Gómez MJ, Martínez-Calle M, Cruz A and Pérez-Gil J (2015) A model for the structure and mechanism of action of pulmonary surfactant protein B. *The FASEB Journal* **29**, 4236–4247.

Olsson U, Camejo G, Hurt-Camejo E, Elfsber K, Wiklund O and Bondjers G (1997) Possible functional interactions of apolipoprotein B-100 segments that associate with cell proteoglycans and the ApoB/E receptor. *Arteriosclerosis Thrombosis and Vascular Biology* **17**, 149–155.

Pattle R (1958) Properties, function, and origin of the alveolar lining layer. *Proceedings of the Royal Society of London. Series B-Biological Sciences* **148**, 217–240.

Pawloski JR, Hess DT and Stamler JS (2005) Impaired vasodilation by red blood cells in sickle cell disease. *Proceedings of the National Academy of Sciences of the United States of America* **102**, 2531–2536.

Pérez-Gil J (2008) Structure of pulmonary surfactant membranes and films: the role of proteins and lipid–protein interactions. *Biochimica et Biophysica Acta (BBA)-Biomembranes* **1778**, 1676–1695.

Pollack GH (2013) The fourth phase of water: a role in fascia? *Journal of Bodywork and Movement Therapies* **17**, 510–511.

Pries AR, Secomb TW and Gaehtgens P (2000) The endothelial surface layer. *Pflugers Archiv* **440**, 653–666.

Reitsma S, Slaaf DW, Vink H, Van Zandvoort MA and Oude Egbrink MG (2007) The endothelial glycocalyx: composition, functions, and visualization. *Pflügers Archiv-European Journal of Physiology* **454**, 345–359.

Richmond P, Davies B and Ninham B (1972) Van der Waals attraction between conducting molecules. *Physics Letters A* **39**, 301–302.

Scarpelli EM (2003) Physiology of the alveolar surface network. *Comparative Biochemistry and Physiology Part A: Molecular & Integrative Physiology* **135**, 39–104.

Secomb TW, Hsu R and Pries AR (1998) A model for red blood cell motion in glycocalyx-lined capillaries. *American Journal of Physiology* **274**(3 Pt 2), H1016–H1022.

Shin S, Mohan S and Fung HL (2011) Intracellular L-arginine concentration does not determine NO production in endothelial cells: implications on the 'L-arginine paradox'. *Biochemical and Biophysical Research Communications* **414**, 660–663.

Squire JM, Chew M, Nneji G, Neal C, Barry J and Michel C (2001) Quasi-periodic substructure in the microvessel endothelial glycocalyx: a possible explanation for molecular filtering? *Journal of Structural Biology* **136**, 239–255.

Thi MM, Tarbell JM, Weinbaum S and Spray DC (2004) The role of the glycocalyx in reorganization of the actin cytoskeleton under fluid shear stress: a 'bumper-car' model. *Proceedings of the National Academy of Sciences* **101**, 16483–16488.

van Oosten AS and Janmey PA (2013) Extremely charged and incredibly soft: physical characterization of the pericellular matrix. *Biophysical Journal* **104**, 961–963.

Vukosavljevic N, Jaron D, Barbee KA and Buerk DG (2006) Quantifying the L-arginine paradox *in vivo*. *Microvascular Research* **71**, 48–54.

Yurchenko SO, Shkirin AV, Ninham BW, Sychev AA, Babenko VA, Penkov NV, Kryuchkov NP and Bunkin NF (2016) Ion-specific and thermal effects in the stabilization of the gas nanobubble phase in bulk aqueous electrolyte solutions. *Langmuir* **32**, 11245–11255.